6

Stability Analysis: Linear Approaches

6.1 STABILITY AND TRANSIENT RESPONSE

The concept of stability is best explained by referring to the illustration in Figure 6.1. The four plots in this figure represent the impulse responses from a linear system under different conditions. In case (a), the response is similar to that exhibited by an overdamped or critically damped system. In case (b), the system exhibits an underdamped response, i.e., there is some oscillation in the response but it is eventually damped out. In both cases, the system is said to be *stable*. However, in case (d), the impulsive stimulus produces a response that is oscillatory with growing amplitude; as a consequence, the system output never returns to its original operating point prior to stimulation. This is the hallmark of an *unstable* system. With these examples in mind, we introduce the following definition of stability: *a stable dynamic system is one that will respond to a bounded input with a bounded response.* Apart from the clear-cut cases of "stable" and "unstable" systems, there are *conditionally or marginally stable* systems that exhibit undamped oscillations (e.g. case (c)). Here, the response is bounded but never returns to the steady operating level prior to perturbation; however, such systems can exhibit unbounded responses if stimulated with certain bounded inputs, such as sinusoidal waves with frequencies that match the characteristic frequencies of the system.

We examined in considerable detail in Chapter 4 how first-order and second-order systems, operating in either open-loop or closed-loop modes, respond to impulsive or step inputs. Recall that the dynamics of the system responses, i.e., the "transient responses," were determined by the roots of the denominator, or the *poles*, of the model transfer function. For the closed-loop ($k > 0$) generalized second-order system, this was shown in Equation (4.51) to be:

$$\frac{Y(s)}{X(s)} = \frac{G_{SS}\omega_n^2}{s^2 + 2\zeta\omega_n s + (1 + kG_{SS})\omega_n^2} \tag{6.1}$$

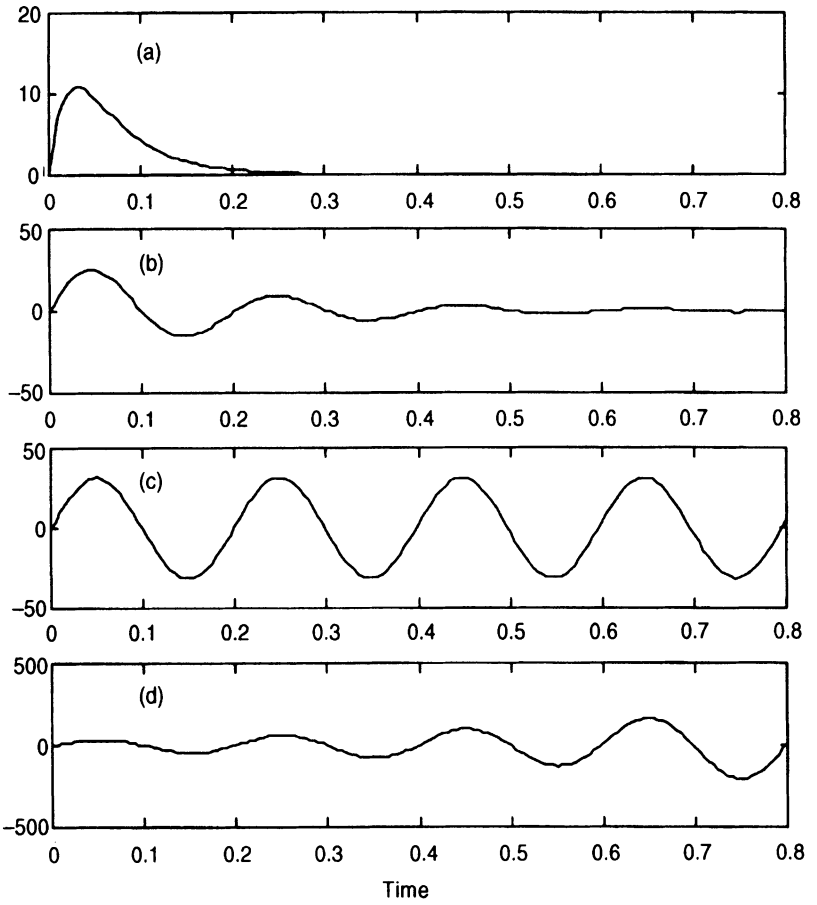

Figure 6.1 Responses of a system that is (a) stable and overdamped; (b) stable and underdamped; (c) marginally stable or oscillatory; (d) unstable.

so that the system poles are given by the roots (α_1 and α_2) of

$$s^2 + 2\zeta\omega_n s + (1 + kG_{SS})\omega_n^2 = 0 \tag{6.2}$$

i.e.,

$$\alpha_{1,2} = -\zeta\omega_n \pm \omega_n\sqrt{\zeta^2 - (1 + kG_{SS})} \tag{6.3}$$

The poles can be real, imaginary or complex, depending on the size of ζ^2 relative to the term $1 + kG_{SS}$, as shown by Equation (6.3). Thus, the impulse response corresponding to Equation (6.1) is given by

$$h(t) = \frac{G_{SS}\omega_n^2}{\alpha_2 - \alpha_1}\left(e^{\alpha_2 t} - e^{\alpha_1 t}\right) \tag{6.4}$$

For positive values of ζ, ω_n, k and G_{SS}, Equation (6.4) shows that the transient response will take on one of the forms represented in cases (a), (b), and (c) in Figure 6.1, but not case (d). This arises from the fact that in cases (a), (b), and (c), the real parts of the roots are either negative or zero, so that the terms within the parentheses in Equation (6.4) represent

exponential decaying, exponentially damped, or simply sinusoidal dynamics. The exponentially growing behavior of the *unstable* system would only occur *if the real parts of* α_1 *and/or* α_2 *were positive.* This could be so if ζ or ω_n were negative; however, this would not be physically feasible. The only possible way in which the closed-loop model represented by Equation (6.1) could realistically be made unstable would be by making k negative, i.e. with positive feedback. If k were to be negative and to assume a magnitude larger than $1/G_{SS}$, one of the roots in Equation (6.3) would start to become positive real, and the resulting impulse response (Equation (6.4)) would increase exponentially with time.

We can summarize the conclusions from the above discussion on stability by extending the results to more generalized systems of the forms shown in Figure 6.2. In Figure 6.2a, the dynamics of the forward and feedback components are characterized by transfer functions $P(s)$ and $Q(s)$, respectively. The gain of the forward path is controlled by the static factor K, which can be varied between zero and infinity. Figure 6.2b shows a similar configuration except that, here, the feedback gain can be varied by varying K between zero and infinity. For the kind of system represented in Figure 6.2a, the closed-loop transfer function is

$$H_A(s) = \frac{Y(s)}{X(s)} = \frac{KP(s)}{1 + KP(s)Q(s)} \tag{6.5}$$

For the type of system shown in Figure 6.2b, the closed-loop transfer function is

$$H_B(s) = \frac{Y(s)}{X(s)} = \frac{P(s)}{1 + KP(s)Q(s)} \tag{6.6}$$

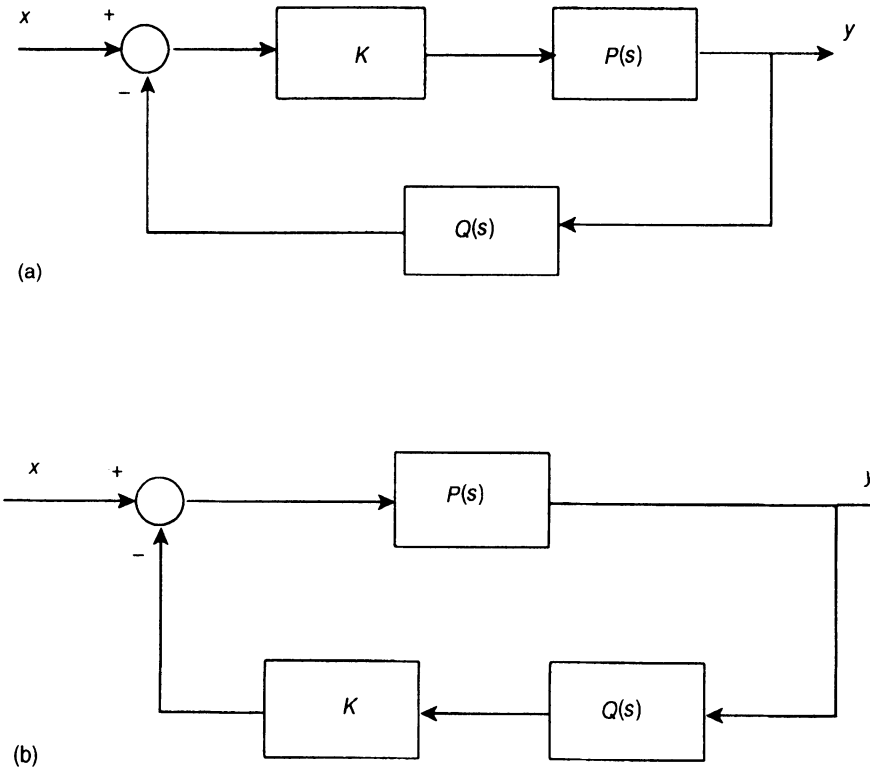

Figure 6.2 Closed-loop systems with variable forward (a) and feedback (b) gains.

Note that, in both cases, the denominator of the closed-loop transfer function is the same. Thus, for given forms of $P(s)$ and $Q(s)$ and gain K, both types of systems will have the same transient response. As in the example of the lung mechanics model, the transient response and stability of both these systems are determined by the poles of their closed-loop transfer functions, i.e., the roots of the following characteristic equation:

$$1 + KP(s)Q(s) = 0 \tag{6.7}$$

Note that the product $KP(s)Q(s)$ yields the *loop transfer function* $\{LG(s)\}$ of both closed-loop systems. (Recall from Section 3.2 that the magnitude of $LG(s)$ is the *loop gain* of the feedback control system.) Thus, Equation (6.7) can be generalized further to

$$1 + LG(s) = 0 \tag{6.8}$$

Extending the result arrived at earlier, we can conclude that, in each of the closed-loop systems shown in Figure 6.2, the transient response will be unstable if the *real part of any root* of its characteristic equation (Equation (6.7)) becomes *positive*.

6.2 ROOT LOCUS PLOTS

The root locus method is a classical procedure used to determine how the poles of the closed-loop transfer function would change as a function of a system parameter (generally, some gain constant), given the location of the open-loop poles and zeros. In fact, the "root locus" is the path on the complex s-plane traced by the closed-loop poles when the system parameter in question varies over a range of values. To illustrate how this method is applied, we turn once again to our simple lung mechanics model. Referring back to Figure 4.2b, we find that the lung mechanics model is merely a special case of the closed-loop form shown in Figure 6.2, where

$$P(s) = \frac{1}{LCs^2 + RCs + 1} \tag{6.9}$$

$$Q(s) = 1 \tag{6.10}$$

and

$$K = k \tag{6.11}$$

For given values of the lung mechanics parameters (L, C, and R), the root locus will show us how the dynamic behavior of the model changes as the feedback gain takes on a range of values. Applying Equation (6.7), the task then is to solve for the roots of the following characteristic equation as k varies:

$$1 + \frac{k}{LCs^2 + RCs + 1} = 0 \tag{6.12}$$

This is equivalent to solving

$$LCs^2 + RCs + 1 + k = 0 \tag{6.13}$$

The general solution for the roots of Equation (6.13) is

$$\alpha_{1,2} = \frac{-R \pm \sqrt{R^2 - 4L(1+k)/C}}{2L} \tag{6.14}$$

To solve Equation (6.14), we will assume, as in Section 4.3, that $L = 0.01$ cm $H_2O\,s^2\,L^{-1}$, $C = 0.1$ L cm H_2O^{-1}, and $R = 1$ cm $H_2O\,s\,L^{-1}$. It is generally useful to determine the locations of the closed-loop poles when k assumes its two most extreme values. First, note that when $k = 0$, solving Equation (6.13) becomes equivalent to determining the locations of the poles of the open-loop system, $P(s)$. Substituting the above values of L, C, R, and k into Equation (6.14), we obtain the following solutions: $\alpha_1 = -88.73$ and $\alpha_2 = -11.27$. For these parameter values, both poles are real and negative. At the other extreme, when k becomes infinitely large, then Equation (6.14) yields the solutions: $\alpha_1 = -50 + j\infty$ and $\alpha_2 = -50 - j\infty$. Thus, for very large k, the poles are complex. Finally, the value of k at which the two real poles become complex can be found by solving for the value of k where the expression inside the square-root operation in Equation (6.14) goes to zero, i.e.,

$$k = \frac{R^2C}{4L} - 1 \tag{6.15}$$

Substituting in values for L, R, and C, we obtain $k = 1.5$.

The complete root locus plot of the system in question can be obtained easily with the use of the MATLAB Control System Toolbox function "`rlocus`." This function assumes that the product $P(s)Q(s)$ yields a transfer function H that takes the form of the ratio of two polynomial functions of s:

$$P(s)Q(s) = H(s) = \frac{N(s)}{D(s)} \tag{6.16}$$

Then, Equation (6.7) can be recast into the following form:

$$D(s) + KN(s) = 0 \tag{6.17}$$

"`rlocus`" finds the solution to Equation (6.17) for all values of K between 0 and infinity. For our specific example, the following MATLAB command lines can be used to plot the corresponding root locus:

```
>> Ns = [1];
>> Ds =[L*C R*C} 1];
>> Hs = tf(Ns, Ds);
>> rlocus(Hs);
```

The resulting root locus plot is displayed in Figure 6.3. Note that the locations of the closed-loop poles when k equals zero, 1.5, and infinity are exactly as we had deduced earlier. Also, since the poles always lie on the left-hand side of the s-plane (i.e., real parts of poles are always negative), the closed-loop system is stable for all positive values of feedback gain, k. Note that the root locus gives us a good global picture of the transient response characteristics of the system but tells us little about its frequency response.

As a further example, we consider the linear lung mechanics model when integral feedback control is employed instead of proportional feedback, i.e., in this case, the fluctuations in alveolar pressure are integrated before being fed back to the comparator.

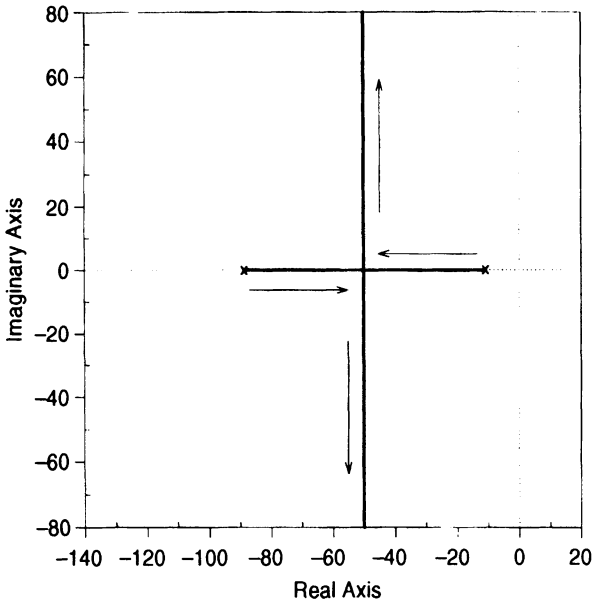

Figure 6.3 Root locus plot for the lung mechanics model with proportional feedback. Locations marked " × " indicate positions of poles when $k = 0$. Arrows indicate direction in which the poles move as k is increased from zero to infinity. Dotted horizontal and vertical lines represent the real and imaginary axes, respectively.

This system is displayed in Figure 6.4. Referring to Figure 6.2b, the forward transfer function $P(s)$ remains the same while the feedback transfer function $Q(s)$ is now given by

$$Q(s) = \frac{1}{s} \tag{6.18}$$

The characteristic equation (Equation (6.17)) now assumes the specific form

$$LCs^3 + RCs^2 + s + k = 0 \tag{6.19}$$

The above equation can be solved easily using MATLAB by simply inserting an extra term into the row vector `Ds` that represents $D(s)$:

```
>> Ns = [1];
>> Ds = [L*C R*C} 1 0];
>> Hs = tf(Ns, Ds);
>> rlocus(Hs);
```

The corresponding root locus plot, displayed in Figure 6.5, shows a form that differs significantly from the plot in Figure 6.3. Because the characteristic equation is now third-order, there are three poles instead of two. When $k = 0$, all three poles are located on the real axis, one of which is situated at the origin ($s = 0$). As k increases, the most negative pole becomes progressively more negative while remaining real. However, when k increases beyond 2.64, the other two poles become complex, i.e., the transient response becomes a damped oscillation that becomes less and less damped, and the frequency of which progressively increases, as k continues to increase. Finally, when k exceeds 100, the system becomes unstable as these two poles move into the right-hand side of the s-plane, i.e., the impulse response assumes the form of a growing oscillation. These results

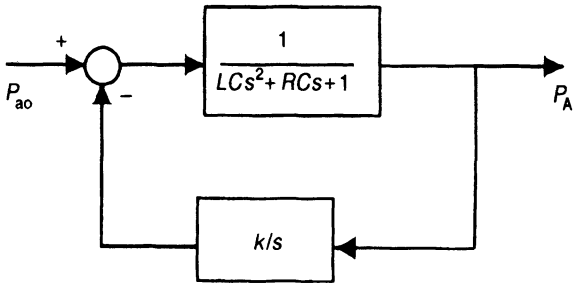

Figure 6.4 Linear lung mechanics model with integral feedback.

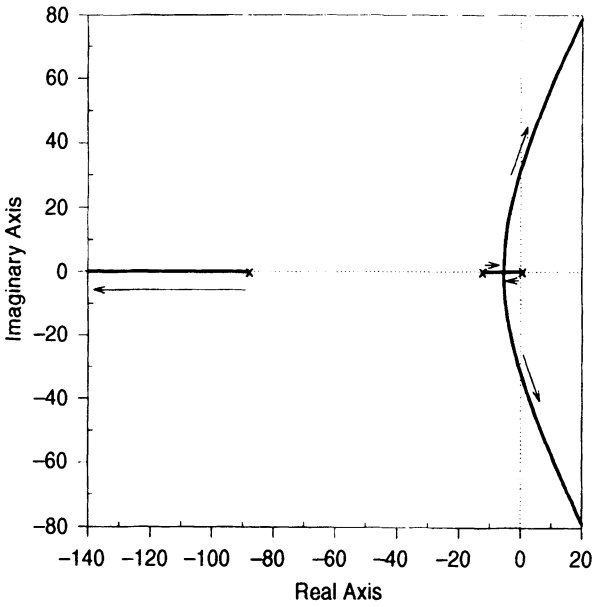

Figure 6.5 Root locus plot for the lung mechanics model with integral feedback. Poles at $k = 0$ are marked "×". Arrows indicate direction in which the three poles move as k is increased toward infinity.

demonstrate that the integral feedback system depicted here exhibits dynamics that are less stable than the proportional feedback case, although it gives a faster response.

6.3 ROUTH–HURWITZ STABILITY CRITERION

The root locus method requires the evaluation of all roots of the characteristic equation in order to determine whether a given system is stable or unstable. The Routh–Hurwitz technique is a classical stability test that enables such a determination without the need to actually evaluate the roots. With the computational tools that are available nowadays, this test has become somewhat obsolete. Nonetheless, we will describe it here for the sake of completeness.

We assume the following general form for the characteristic equation of the closed-loop system in question:

$$a_n s^n + a_{n-1} s^{n-1} + \cdots + a_1 s + a_0 = 0 \tag{6.20}$$

The Routh–Hurwitz technique requires the computation of values based on the coefficients of the characteristic equation and the arrangement of these values into an array of the following construction (with each row corresponding to a power of s, as indicated in the margin to the left of the array):

$$\begin{array}{c|cccc} s^n & a_n & a_{n-2} & a_{n-4} & \cdot \\ s^{n-1} & a_{n-1} & a_{n-3} & a_{n-5} & \cdot \\ s^{n-2} & b_1 & b_2 & b_3 & \cdot \\ s^{n-3} & c_1 & c_2 & c_3 & \cdot \\ \cdot & \cdot & \cdot & \cdot & \cdot \\ s^1 & p_1 & & & \\ s^0 & q_1 & & & \end{array} \tag{6.21}$$

where

$$b_1 = \frac{a_{n-1}a_{n-2} - a_n a_{n-3}}{a_{n-1}}, \qquad b_2 = \frac{a_{n-1}a_{n-4} - a_n a_{n-5}}{a_{n-1}}.$$
$$c_1 = \frac{b_1 a_{n-3} - b_2 a_{n-1}}{b_1} \tag{6.22}$$

and so on. The Routh–Hurwitz criterion states that the number of closed-loop poles located on the right-hand side of the s-plane is given by the number of changes in sign in the first column of the constructed array in Equation (6.21). Thus, for a *stable* system, there should be *no changes in sign in the first column of the array.*

To illustrate the use of the Routh–Hurwitz test, we will apply it to the two examples discussed in Section 6.2. Consider first the linear lung mechanics model with proportional feedback. The characteristic equation here is given by Equation (6.13). Using Equation (6.21), the Routh array is

$$\begin{array}{c|cc} s^2 & LC & 1+k \\ s & RC & 0 \\ s^0 & 1+k & 0 \end{array} \tag{6.23}$$

For positive values of L, C, and R and for $k \geq 0$, there are no changes in sign in the terms of the *first column* of the array. Therefore, by the Routh–Hurwitz criterion, the system defined by Equation (6.13) will always be stable.

In the lung mechanics model with integral feedback, the characteristic equation is given by Equation (6.19). In this case, the first two columns of the Routh array are

$$\begin{array}{c|cc} s^3 & LC & 1 \\ s^2 & RC & k \\ s & 1 - \dfrac{Lk}{R} & 0 \\ s^0 & k & 0 \end{array} \tag{6.24}$$

For positive values of L, C, R, and k, note that all terms in the first column of Equation (6.24) will be positive, except for the third term which can become negative if

$$k > \frac{R}{L} \tag{6.25}$$

For $R = 1\ \text{cm H}_2\text{O s L}^{-1}$ and $L = 0.01\ \text{cm H}_2\text{O s}^2\ \text{L}^{-1}$, Equation (6.25) predicts that there will be one change of sign in Equation (6.24) when k exceeds the value of 100. This is exactly the result obtained in Section 6.2 when we employed the root locus method.

6.4 NYQUIST CRITERION FOR STABILITY

One primary disadvantage of the Routh–Hurwitz test is that it becomes difficult to apply when the characteristic equation cannot be simply expressed as a polynomial function of s. Pure time delays are found abundantly in physiological systems. Although these can be approximated by rational polynomial expressions (see Problem P4.3), the resulting characteristic equation can become extremely unwieldy. For these kinds of problems, it is generally more convenient to employ the Nyquist stability test.

The formal mathematical development of the Nyquist stability criterion will not be presented here, as it involves a fair bit of complex variable theory; the interested reader can find this in most engineering texts on control systems. Instead, we will employ a more intuitive approach by illustrating the basic notions underlying this criterion. Consider the very simple negative feedback system shown in Figure 6.6. The input, u, represents a disturbance to the system that is nonzero for only a brief period of time. The system output, x, is fed back through a static gain $-K$ and added to the input before being fed forward through the time-delay (T_D) block. Note that the negativity in feedback control is implemented through the assignment of a negative value to the feedback gain and the addition (not subtraction) of the resulting feedback signal (z) at the level of the summing junction.

Figure 6.7 shows three of the many possibilities with which the system responds following the imposition of a transient disturbance, u. In all these cases, we have assumed that u takes the form of a half-sine wave. Consider case (a) in which we assume $K = 0.5$ and T_D is half the duration of u. Here, the initial passage of u through the forward and feedback blocks produces an inverted and attenuated (by 50%) half-sine wave at z, labeled 1 in Figure 6.7a (upper panel). Propagation of this signal around the loop a second time would produce a response at z of the form labeled as 2. Similarly, the third and fourth traversals around the entire loop would produce 3 and 4, respectively. This process would continue until the "echoes" of the initial u are finally damped out totally. Each time there is a complete traversal around the loop, there is a change in sign, reflecting the negative nature of the feedback. Superimposition of all these individual effects on the initial disturbance leads to the complete response at x shown in the lower panel of Figure 6.7a. Thus, the system response to u is a rapidly damped oscillation, i.e., the system in this case is stable. In Figure 6.7b, K is assigned the value of 0.5 again, but T_D is now increased to a value equal to the duration of u. This produces the responses in z labeled as 1 after the first traversal around the loop and 2 after the second traversal (Figure 6.7b, upper panel). The net result again is a damped oscillation (Figure 6.7b, lower panel). However, in this case, the oscillation appears to be more slowly damped and the frequency of the oscillation is also lower. Note also, that the corrective actions (1 in response to u and 2 in response to 1) have been delayed so much that they occur

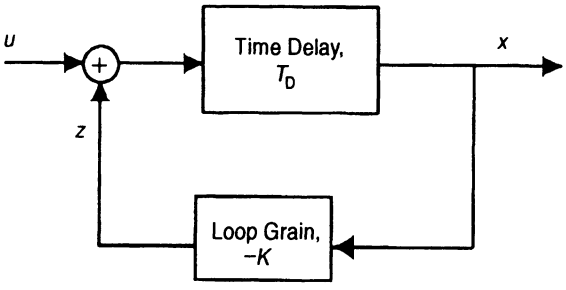

Figure 6.6 Simple negative feedback system with delay. Note that, in this example, the negativity in feedback is embedded in the "loop gain" block.

out of phase (i.e., at 180°) with the preceding fluctuations. Finally, in case (c), the time delay is kept the same as that for case (b), but the loop gain magnitude is increased to 1. As in case (b), due to the increased delay, the feedback signal tends to reinforce the effect of the initial disturbance rather than to cancel it out. However, in this case, since there is no attenuation in the feedback loop, the net result is a sustained oscillation of period equal to twice the length of T_D. It is easy to see that if the loop gain were to be increased further to a value exceeding 1, the system response would be an oscillation with growing amplitude.

From the examples shown in Figure 6.7, it is clear that a closed-loop system can become unstable if the total phase lag imposed by all system components around the loop equals 180° *and* the loop gain magnitude is at least unity. This is the basic notion underlying the Nyquist criterion. Thus, in order to determine whether a specific closed-loop system is stable or unstable, we would first deduce the *loop transfer function* (i.e., the product of all component transfer functions around the closed loop). The Nyquist plot of the loop transfer function is generated. Note that a loop gain of unit magnitude and phase lag of 180° is represented by the point $(-1 + j0)$ on the complex plane. *The system is stable if the* $(-1 + j0)$ *point lies to the left of the Nyquist plot as the locus is traversed in the direction of increasing*

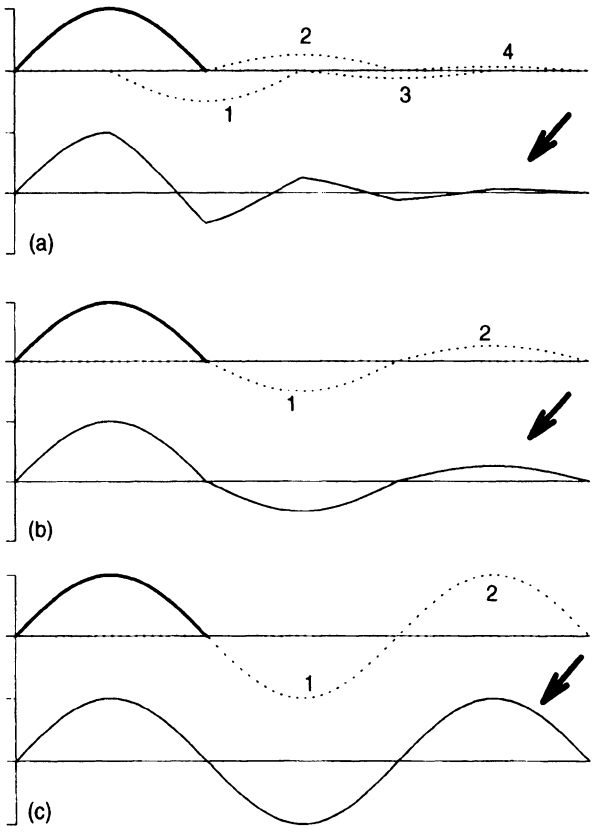

Figure 6.7 Response of the negative feedback system with delay to an initial disturbance when: (a) loop gain magnitude < 1 and phase lag < 180°; (b) loop gain magnitude < 1 and phase lag = 180°; and (c) loop gain magnitude = 1 and phase lag = 180°.

frequency. Another way of stating this criterion is that in the stable system the Nyquist plot *will not encircle* the $(-1 + j0)$ point. In order to make this determination, it is generally necessary to evaluate the loop transfer function from zero frequency to infinity, or at least over a wide band of frequencies. This criterion, as stated above, is valid as long as the loop transfer function does not contain any poles with positive real parts. If this condition does not apply, one has to employ a different version of the Nyquist criterion; more details of the method under such circumstances can be found elsewhere (e.g., Dorf and Bishop, 1995).

The reader may recall that the Nyquist representation was previously discussed in Section 5.2.3. However, one should be cautioned that, in Chapter 5, the examples shown were those in which we characterized the frequency responses corresponding to the open-loop and closed-loop transfer functions of the systems in question. For a determination of stability, we need to evaluate the *loop transfer function*, which will yield a Nyquist plot quite different from the Nyquist plots that correspond to the open-loop or closed-loop transfer functions of the same system.

To illustrate the application of the Nyquist stability criterion, we turn once again to the two examples that have been discussed earlier. For the linear lung mechanics model with proportional feedback, the loop transfer function, $H_{L1}(s)$, is given by

$$H_{L1}(s) = \frac{k}{LCs^2 + RCs + 1} \tag{6.26}$$

The frequency response corresponding to Equation (6.26) is obtained by substituting $j\omega$ for s:

$$H_{L1}(\omega) = \frac{k}{(1 - LC\omega^2) + jRC\omega} \tag{6.27}$$

The Nyquist plots corresponding to Equation (6.27) are shown in Figure 6.8 for three values of feedback gain ($k = 1$, 10, and 100). Note that at $\omega = 0$, $H_{L1}(\omega) = k$. However, the zero frequency values for $H_{L1}(\omega)$ when $k = 10$ and $k = 100$ lie outside the range displayed. In Equation (6.27), also notice that when $\omega \to \infty$, $H_{L1}(\omega) \to 0$. Thus, for each plot, the Nyquist locus begins at the point $(k + j0)$ at zero frequency and ends at the origin at infinite frequency. The direction of traversal of each locus with increasing values of frequency is indicated by the arrows (Figure 6.8). Except for the hypothetical case when k becomes infinite, it can be seen that none of the Nyquist loci touch or encircle the $(-1 + j0)$ point (represented as the filled circle in Figure 6.8). Thus, this system is stable for all finite values of feedback gain.

The loop transfer function for the linear lung mechanics model with integral feedback, $H_{L2}(s)$, is given by

$$H_{L2}(s) = \frac{k}{LCs^3 + RCs^2 + s} \tag{6.28}$$

The frequency response corresponding to the above transfer function is

$$H_{L2}(\omega) = \frac{k}{-RC\omega^2 + j\omega(1 - LC\omega^2)} \tag{6.29}$$

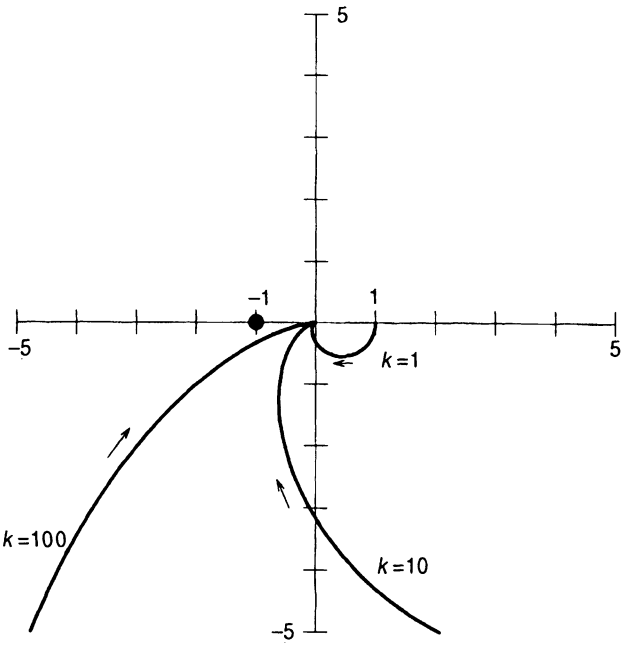

Figure 6.8 Nyquist plots for the linear lung mechanics model with proportional feedback. Feedback gains shown are $k = 1$, 10 and 100. For the latter two cases, only portions of the Nyquist plots lie outside of the scale shown. Arrows indicate direction of Nyquist trajectories as frequency increases from 0 to infinity. Filled circle represents location of the $-1 + j0$ point.

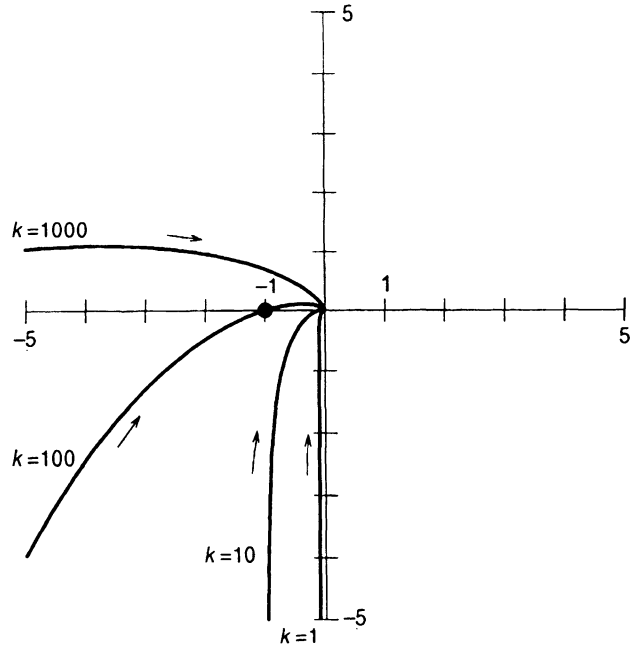

Figure 6.9 Nyquist plots for the linear lung mechanics model with integral feedback. In all cases ($k = 1$, 10, 100, 1000), portions of the Nyquist plot lie outside of the scale shown. Arrows indicate the direction of Nyquist trajectories as frequency increases from 0 to infinity. Filled circle represents location of the $-1 + j0$ point.

In this case, note that when $\omega \to 0$, $H_{L2}(\omega) \to -j\infty$. When ω is very large, the term in ω^3 will become much more important than the other terms in the denominator in Equation (6.29). Thus, when $\omega \to \infty$, $H_{L2}(\omega) \to 0$, with the Nyquist locus at high values of ω tending to approach the origin along the positive imaginary axis. Figure 6.9 shows the behavior of Nyquist loci at four different values of feedback gain ($k = 1$, 10, 100, and 1000). All loci start off from $-j\infty$ and curve in toward the origin as frequency increases toward infinity. For values of k below 100, the Nyquist loci remain to the right of the $(-1 + j0)$ point, so the system remains stable. When $k = 100$, the Nyquist locus passes through the $(-1 + j0)$ point, indicating that the system becomes conditionally stable in this condition. Then, when $k > 100$, the system becomes unstable with the Nyquist plot encircling the $(-1 + j0)$ point.

6.5 RELATIVE STABILITY

While it is useful to be able to determine under what conditions a closed-loop system would become marginally stable or unstable, it is equally useful to have a means of assessing how "far" the point of instability is from the current state of system stability. Consider two stable systems. Suppose the effect of an impulsive disturbance elicits a rapidly damped, nonoscillatory response from the first system while the same disturbance produces an underdamped oscillatory response from the second system. Although both systems are "stable," it would be reasonable to conclude that the first may be considered "more stable" than the second. This is the basis underlying the notion of *relative stability.*

The relative stability of a given system can be quantified in terms of either the *gain margin* or the *phase margin.* Both provide measures of the $(-1 + j0)$ point from specific points on the locus of the loop transfer function. The *gain margin* refers to the *factor by which the loop gain corresponding to a phase of* $-180°$ *has to be increased before it attains the value of unity.* The frequency at which the phase of the loop transfer function becomes $-180°$ is known as the *phase crossover frequency.* To illustrate this point, consider a special case of the linear lung mechanics model with integral feedback that has the following specific loop transfer function:

$$H_{L2}(s) = \frac{1}{s^3 + 3s^2 + 2s} \tag{6.30}$$

The Bode magnitude and phase plots corresponding to Equation (6.30) are displayed in Figure 6.10. Note that at the phase crossover frequency, ω_{pc}, when the phase of $H_{L2}(\omega_{pc})$ becomes equal to $-180°$, the gain of $H_{L2}(\omega_{pc})$ remains less than unity, implying that this system is stable. By definition, the gain margin (GM) in this case is given by

$$|H_{L2}(\omega_{pc})| \times GM = 1 \tag{6.31}$$

Therefore, the gain margin, expressed in decibels, is

$$GM_{dB} = 20 \log_{10}\left(\frac{1}{|H_{L2}(\omega_{pc})|}\right) = -20 \log_{10}|H_{L2}(\omega_{pc})| \tag{6.32}$$

As shown in the top panel of Figure 6.10, GM_{dB} is given by the vertical distance between the 0 dB axis and the point on the gain plot at which the phase crossover frequency is attained.

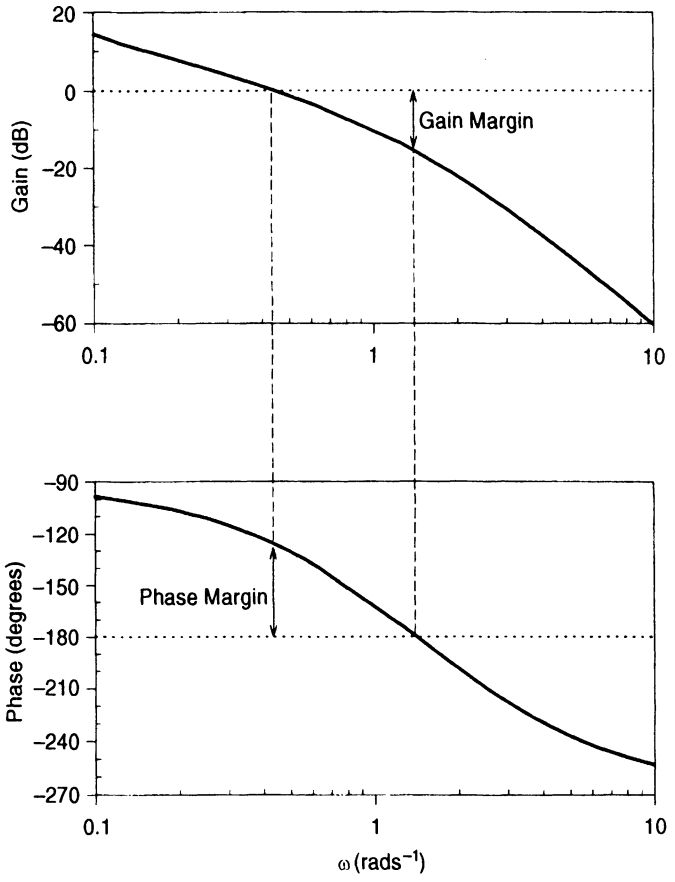

Figure 6.10 Derivation of gain and phase margins from the Bode plots of the loop transfer function.

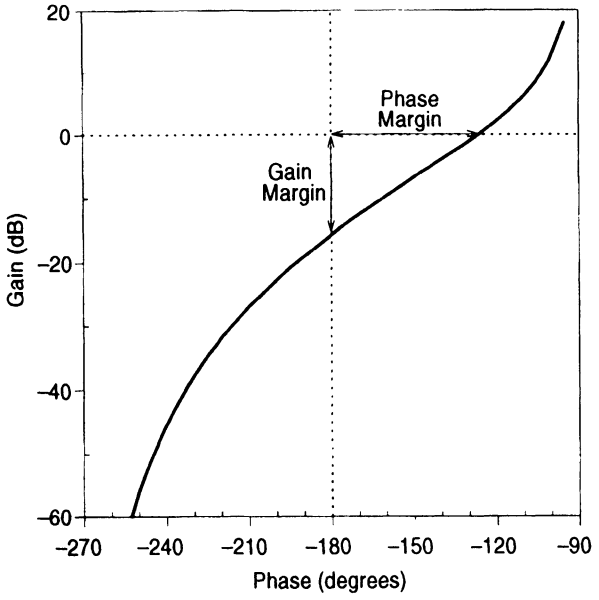

Figure 6.11 Derivation of gain and phase margins from the Nichols chart of the loop transfer function.

The other measure of relative stability, the *phase margin*, is defined as the *shift in phase at unit loop gain necessary to produce a phase lag of* 180°. The frequency at which the loop gain becomes equal to unity is known as the *gain crossover frequency* (ω_{gc}). Referring to the lower panel of Figure 6.10, note that the phase margin is given by the vertical distance between the $-180°$ line and the point on the Bode phase plot at which the gain crossover frequency is attained.

The gain and phase margins can also be readily deduced from the Nichols chart (Figure 6.11) and the Nyquist plot (Figure 6.12). In the case of the Nyquist plot, the intersection between the Nyquist locus and the negative horizontal axis yields $|H_{L2}(\omega_{pc})|$ which, by Equation (6.31), gives the reciprocal of *GM*. Note, however, that here *GM* is expressed as a ratio and not in terms of decibels. It can be appreciated from Figures 6.10 through 6.12 that larger positive values for the gain or phase margins imply greater relative stability. On the other hand, negative values for either gain or phase margins would imply that the system in question is already unstable.

Numerical evaluation of the gain and phase margins can be performed easily using the function `margin` in the MATLAB Control System Toolbox. For instance, to evaluate the gain and phase margins for the loop transfer function defined by Equation (6.30), the following MATLAB command lines (contained in script file "`gpmargin.m`") may be applied:

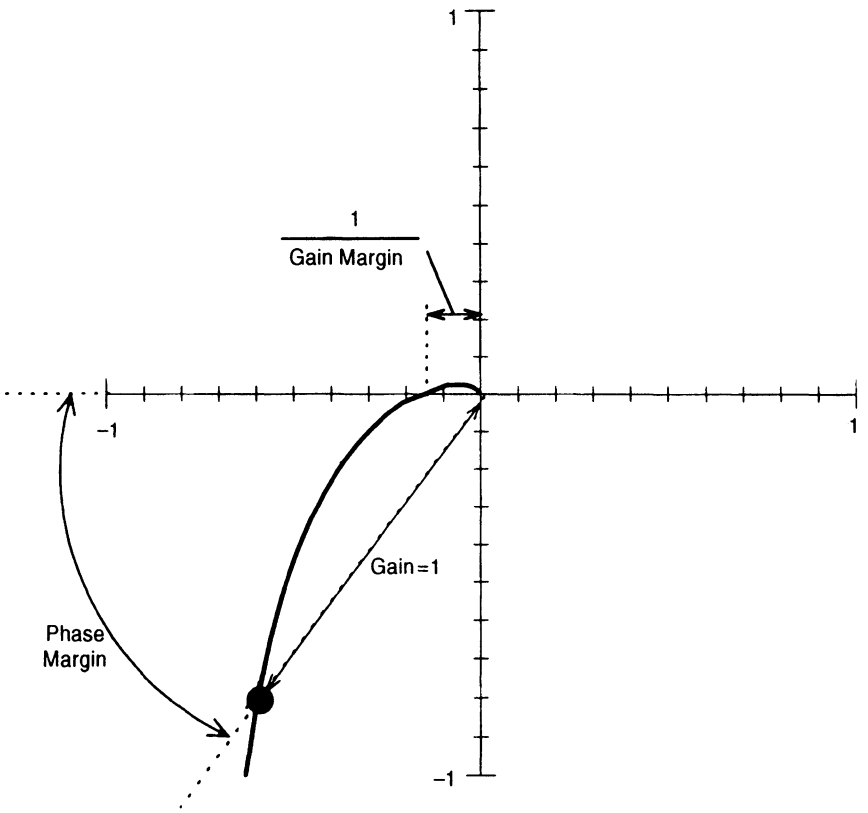

Figure 6.12 Derivation of gain and phase margins from the Nyquist plot of the loop transfer function.

```
>>% First construct loop transfer function and vector of frequencies
>> num = [1];
>> den = [1  3  2  0];
>> Hs = tf(num, en);
>> f = 0.01:0.01:10;
>> w = 2*pi*f;

>>% Compute magnitude (mag) and phase (pha) of loop transfer function
>> [mag, pha] = bode(Hs, w)

>>% Compute gain margin (GM), phase margin (PM), gain crossover
>>% frequency (wcG) and phase crossover frequency (wcP)
>> [GM, PM, wcG, wcP] = margin (mag, pha, w);

>>% Plot Bode diagram showing gain and phase margins
>> margin(mag,pha,w);
```

6.6 STABILITY ANALYSIS OF THE PUPILLARY LIGHT REFLEX

The pupillary light reflex has been studied extensively using control system analysis, most notably by bioengineering pioneers Lawrence Stark and Manfred Clynes. The purpose of this reflex is to regulate the total light flux reaching the retina, although the same pupil control system is also used to alter the effective lens aperture so as to reduce optical aberrations and increase depth of focus. The reflex follows the basic scheme shown in Figure 6.13a. An

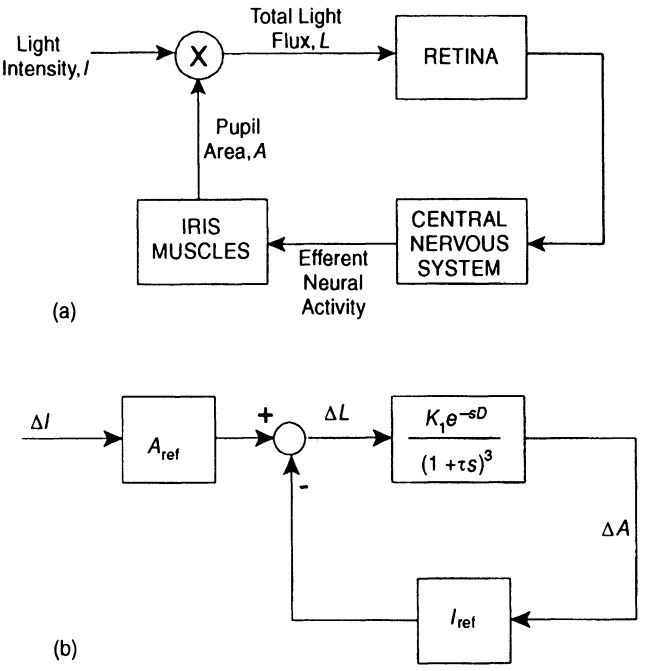

Figure 6.13 (a) Functional scheme for the pupillary control system. Note that the total light flux, L, is given by the product of light intensity, I, and pupil area, A. (b) Linearized (small-signal) model of the pupillary light reflex.

increase in the intensity (I) of ambient light elevates the total light flux (L) received by the retina, which converts the light into neural signals. The afferent neural information is sent via the optic nerve to the lateral geniculate body and then to the pretectal nucleus. Subsequently, the Edinger–Westphal nucleus sends efferent neural signals back toward the periphery to the iris sphincter and dilator muscles which, respectively, contract and relax to reduce the pupil area (A).

Not surprisingly, quantitative investigations into this feedback control scheme have revealed significant nonlinearities in each of the system components. However, Stark came up with a linear characterization that provides a reasonably good approximation of the underlying dynamics when the changes involved are relatively small. This linearized model is schematized in Figure 6.13b. Using an ingenious experimental design (see Figure 7.13), he was able to functionally "open the loop" of this reflex and measure the dynamics of this system. (This technique is discussed further in Section 7.4.5.) He found that the dynamics could be modeled by a third-order transfer function with time constant τ, in series with a pure time delay D. In Figure 6.13b, ΔI represents a small change in light intensity from the reference intensity level, I_{ref}, while ΔA represents the corresponding change in pupil area from the reference value, A_{ref}, and ΔL is the change in total light flux reaching the retina. Based on the model, the closed-loop transfer function of the pupillary reflex can be deduced as

$$\frac{\Delta A}{\Delta I} = \frac{\dfrac{A_{\text{ref}} K_1 e^{-sD}}{(1+\tau s)^3}}{1 + \dfrac{I_{\text{ref}} K_1 e^{-sD}}{(1+\tau s)^3}} \tag{6.33}$$

By inspection of Figure 6.13b and Equation (6.33) above, one can readily infer that the *loop transfer function* of this model is given by

$$H_{\text{L}}(s) = \frac{K e^{-sD}}{(1+\tau s)^3} \tag{6.34}$$

where $K = I_{\text{ref}} K_1$. Therefore, the characteristic equation for the closed-loop model is

$$1 + \frac{K e^{-sD}}{(1+\tau s)^3} = 0 \tag{6.35}$$

From his measurements on normal humans, Stark found the following values for the model parameters: $K = 0.16$, $D = 0.18$ s and $\tau = 0.1$ s. In the next two subsections, we will assume the above values of D and τ in our analyses and determine the critical value of K above which the model becomes unstable.

6.6.1 Routh–Hurwitz Analysis

In Section 6.3, when the Routh–Hurwitz stability criterion was first discussed, application of the test was simple since the examples considered had characteristic equations that could be expressed as polynomials in s. In Equation (6.35) however, the presence of the

time delay complicates matters a little. Llaurado and Sun (1964) suggested that this problem could be circumvented by expanding e^{-sD} as a power series in s:

$$e^{-sD} \approx 1 - Ds + \frac{D^2s^2}{2} - \frac{D^3s^3}{6} \tag{6.36}$$

Substituting the above approximation for e^{-sD} into Equation (6.35) and collecting terms for each power of s, we obtain the following third-order polynomial expression in s:

$$\left(\tau^3 - \frac{KD^3}{6}\right)s^3 + \left(3\tau^3 + \frac{KD^2}{2}\right)s^2 + (3\tau - KD)s + (1 + K) = 0 \tag{6.37a}$$

Inserting the numerical values for D and τ into Equation (6.37a), we obtain

$$(0.001 - 0.000972K)s^3 + (0.03 + 0.0162K)s^2 + (0.3 - 0.18K)s + (1 + K) = 0 \tag{6.37b}$$

The Routh array corresponding to Equation (6.37b) is

$$\begin{array}{c|ccc} s^3 & 0.001 - 0.000972K & 0.3 - 0.18K & 0 \\ s^2 & 0.03 + 0.0162K & 1 + K & 0 \\ s & \dfrac{890 - 431.72K - 19.44K^2}{300 + 162K} & 0 & 0 \\ s^0 & 1 + K & 0 & 0 \end{array} \tag{6.38}$$

The requirement for stability is that all terms in the first column of the above array should have the same sign. Since the term corresponding to s^0 is $1 + K$, and K must be positive, then for the system to be stable, all terms in the first column of the Routh array must also be positive. Thus, the following inequalities have to be satisfied simultaneously:

$$0.001 - 0.000972K > 0 \tag{6.39a}$$

$$0.03 + 0.0162K > 0 \tag{6.39b}$$

$$\frac{890 - 431.72K - 19.44K^2}{300 + 162K} > 0 \tag{6.39d}$$

$$1 + K > 0 \tag{6.39d}$$

From the first inequality (Equation (6.39a)), we find that $K < 10.3$. The second and fourth inequalities are satisfied for all values of K that are greater than zero. In the third inequality, the quadratic expression in the numerator of the left-hand side has to be factorized first. From this, it can be deduced that the inequality is satisfied if $-24.196 < K < 1.996$. Thus, combining this result with that from the first inequality, we conclude that for the closed-loop system to be stable, K must be less than 1.996. Since the average value of K measured by Stark was 0.16, we can conclude from Routh–Hurwitz analysis that the normal pupillary reflex is a highly stable negative feedback system.

6.6.2 Nyquist Analysis

The frequency response, $H_L(\omega)$, corresponding to the loop transfer function can be obtained by substituting $j\omega$ for s in Equation (6.34):

$$H_L(\omega) = \frac{Ke^{-j\omega D}}{(1+j\omega\tau)^3} = \frac{Ke^{-j\omega D}}{(1-3\omega^2\tau^2)+j\omega\tau(3-\omega^2\tau^2)} \tag{6.40}$$

The problem of evaluating the time-delay transfer function in Equation (6.40a) can be approached in a number of ways. One way is to apply the power series expansion approach employed in the previous section. Another possibility is to employ a Padé approximation to the delay, as we had illustrated in Problem P4.2. The first of these methods converts the time-delay transfer function into a polynomial function of s while the second approximates it with a transfer function that consists of the ratio of two polynomials in s. However, a third approach is to express $H_L(\omega)$ in polar form and recognize that the delay will only affect the phase component of the transfer function. MATLAB offers a convenient means of performing this computation over a given range of frequencies. An illustration of this procedure is given in the MATLAB command lines below.

```
>>% Construct undelayed transfer function & evaluate frequency response
>>num =[K]; den = [tau^3 3*tau^2 3*tau 1];
>> Hs} = tf(num, den);
>> [R, I] = nyquist(Hs); I = squeeze(I); R = squeeze(R);

>>% Add delay to results
>> Rdel = real((R + j*I).*exp(-j*w*D));
>> Idel= imag((R + j*I).*exp(-j*w*D));

>>% Plot final Nyquist diagram
>> plot(Rdel,Idel);
```

The complete script file (named "`pupil.m`") for evaluating Equation (6.40) and plotting the Nyquist diagrams is included in the library of MATLAB/SIMULINK files accompanying this book.

Figure 6.14a displays the Nyquist plot for the normal pupil control system with $K = 0.16$, generated using the above MATLAB code and assuming the parameter values, $D = 0.18$ s and $\tau = 0.1$ s. The Nyquist plots corresponding to increased values of K, 1.6 (dotted curve) and 2 (unbroken curve), are shown in Figure 6.14b. Note that the scale of the axes in Figure 6.14b has been increased to cover a substantially larger range of values. It is clear that the pupillary reflex model is unstable when $K = 2$ but stable when $K = 1.6$. Further computations show that the critical value of K for the development of self-sustained oscillations is 1.85. This is slightly smaller than the 1.996 value deduced in Section 6.6.1. However, the critical value arrived at here is probably the more accurate prediction since, in the previous section, an approximation had to be assumed in order to represent the pure-delay transfer function as a power series.

Examination of all the Nyquist plots in Figure 6.14 shows that the intersection of each locus with the negative real axis (i.e., phase $= -180°$) occurs at the same critical frequency,

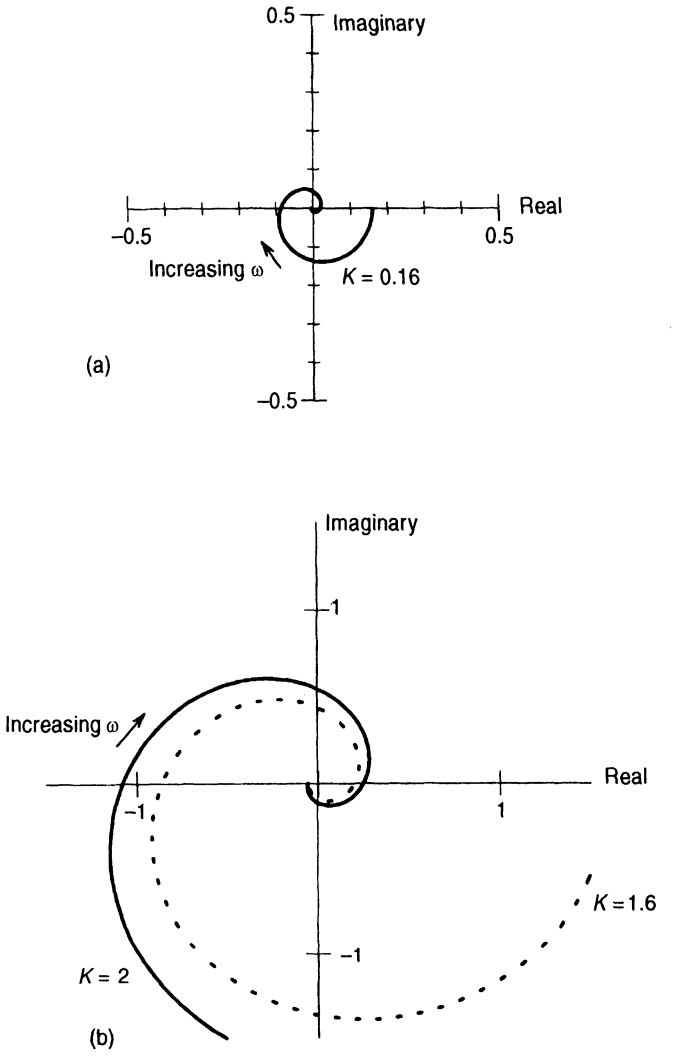

Figure 6.14 Nyquist plots of the linearized pupillary reflex model at (a) normal loop gain factor ($K = 0.16$), (b) elevated loop gain factors ($K = 1.6$ and $K = 2$).

ω_c, regardless of the value of K. This can be confirmed by analysis of the phase of $H_L(\omega)$. At the critical frequency, since the phase of $H_L(\omega)$ must equal $-\pi$ radians (or $-180°$), we have

$$-\pi = -\omega_c D - \tan^{-1}\left(\frac{\omega_c\tau(1-\omega_c^2\tau^2)}{(1-3\omega_c^2\tau^2)}\right) \tag{6.41}$$

Note that ω_c can be deduced by solving Equation (6.41). However, since none of the terms depends on K, ω_c must also be independent of K. ω_c can be found from solution of Equation (6.41) or from inspection of the Nyquist plots to be equal to 7.1 rad s^{-1}, which corresponds to an absolute frequency of 1.1 Hz. This predicted frequency is close to the frequency of continuous oscillations of the pupil, known as "hippus," which have been observed under certain pathological conditions. Stark was able to artificially induce hippus in normal subjects using a clever experimental design. He focused a thin beam of light at the edge of the pupil.

This stimulation of the reflex led to constriction of the pupil, which produced a large decrease in retinal illumination (since much of it was now blocked by the iris). This, in turn, acted through the reflex to dilate the pupil, restoring the effect of the applied retinal illumination. This experimental design was tantamount to elevating the loop gain of the closed-loop system tremendously, thereby setting the stage for a self-sustained oscillation to occur. The frequency of this oscillation was found to be close to that predicted by the model. The good agreement between model prediction and experimental observation supports the approximate validity of the linear assumption in this case.

6.7 MODEL OF CHEYNE–STOKES BREATHING

The term *periodic breathing* refers to the cyclic modulation of respiration that occurs over the time-scale of several breaths. The resulting ventilatory pattern may or may not include periods of apnea, in which breathing ceases altogether. Periodic breathing does not commonly occur in normals during wakefulness; however, its frequency of incidence increases dramatically during ascent to altitude as well as during sleep onset. An exaggerated form of periodic breathing, known as *Cheyne–Stokes breathing*, is frequently observed in patients with congestive heart failure. A large body of evidence suggests that periodic breathing results from an instability in the feedback control system that regulates ventilation and arterial blood gases. In this section, we will demonstrate that this is a reasonable hypothesis by applying stability analysis to a linearized model of chemoreflex regulation of ventilation. Recall that a steady-state nonlinear model for arterial CO_2 and O_2 regulation was discussed previously in Section 3.7. In the present model, we assume that the system is operating under normoxic conditions, so that the chemoreflex response to hypoxia can be ignored. However, the various components of the model are assigned dynamic properties. Since the response of the "central" chemoreceptors located in the ventral medulla is much more sluggish than that of the "peripheral" (carotid body) chemoreceptors, it is convenient to assume that there are functionally two feedback loops in this system: one representing the central chemoreflex and the other representing the peripheral chemoreflex. We also incorporate into the model the delays taken to transport blood from the lungs and the chemoreceptors. A simplified schematic diagram of this dynamic model is shown in Figure 6.15.

6.7.1 CO_2 Exchange in the Lungs

The dynamic equivalent of the gas exchange equation given in Equation (3.48) is

$$V_{\text{lung}} \frac{dP_{\text{ACO}_2}}{dt} = (\dot{V}_{\text{E}} - \dot{V}_{\text{D}})(P_{\text{ICO}_2} - P_{\text{ACO}_2}) + 863Q(C_{\text{vCO}_2} - C_{\text{aCO}_2}) \tag{6.42}$$

where Q represents pulmonary blood flow, V_{lung} is the effective CO_2 storage capacity of the lungs, and C_{aCO_2} and C_{vCO_2} are the CO_2 concentrations in arterial and mixed venous blood, respectively. Other symbols are as defined previously in Section 3.7. It should also be noted that, in the steady state, the last term in Equation (6.42) would equal $863\dot{V}_{\text{CO}_2}$, where $\dot{V}_{\text{CO}_2}$ is the metabolic production rate of CO_2.

Suppose that small perturbations are imposed on $\dot{V}_{\text{E}}$ ($\Delta\dot{V}_{\text{E}}$) and that these lead to small perturbations in P_{ACO_2} (ΔP_{ACO_2}) and C_{aCO_2} (ΔC_{aCO_2}). If we ignore the effect of the arterial blood gas fluctuations on mixed venous CO_2 concentration (since the body tissues represent a very large buffer of CO_2 changes), assume that dead space ventilation remains constant, and

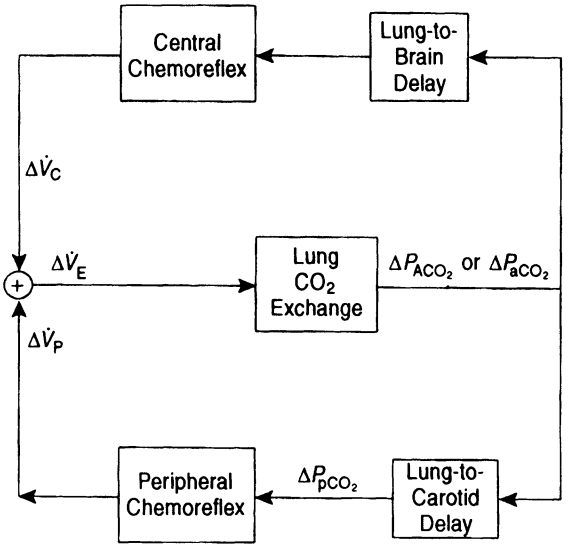

Figure 6.15 Linearized dynamic model of the chemoreflex control of ventilation.

ignore terms involving the product $\Delta\dot{V}_E\,\Delta P_{ACO_2}$, we can derive the following small-signal expression from Equation (6.42):

$$V_{lung}\frac{d(\Delta P_{ACO_2})}{dt} = -(\dot{V}_E - \dot{V}_D)\,\Delta P_{ACO_2} + (P_{ICO_2} - P_{ACO_2})\,\Delta\dot{V}_E - 863Q\,\Delta C_{aCO_2} \quad (6.43a)$$

If we approximate the blood CO_2 dissociation curve with a straight line relating C_{aCO_2} to P_{aCO_2} with slope K_{CO_2}, and impose the assumption of alveolar–arterial P_{CO_2} equilibration, we obtain from Equation (6.43a) the following result:

$$V_{lung}\frac{d(\Delta P_{aCO_2})}{dt} + (\dot{V}_E - \dot{V}_D + 863QK_{CO_2})\,\Delta P_{aCO_2} = (P_{ICO_2} - P_{aCO_2})\,\Delta\dot{V}_E \quad (6.43b)$$

Note that in Equations (6.43a) and (6.43b), $\dot{V}_E$ and P_{aCO_2} represent the steady-state operating levels of minute ventilation and arterial CO_2 tension, respectively. If we take the Laplace transform of Equation (6.43b) and rearrange terms, we can obtain the following expression for the transfer function, $H_{lung}(s)$, of the lungs:

$$H_{lung}(s) \equiv \frac{\Delta P_{aCO_2}}{\Delta\dot{V}_E} = \frac{-G_{lung}}{\tau_{lung}s + 1} \quad (6.44)$$

where

$$\tau_{lung} = \frac{V_{lung}}{\dot{V}_E - \dot{V}_D + 863QK_{CO_2}} \quad (6.45)$$

and

$$G_{lung} = \frac{P_{aCO_2} - P_{ICO_2}}{\dot{V}_E - \dot{V}_D + 863QK_{CO_2}} \quad (6.46)$$

Thus, Equations (6.44) through (6.46) indicate that, under small-signal conditions, the dynamics of CO_2 exchange in the lungs may be modeled approximately as a simple first-order system with time constant τ_{lung} and gain G_{lung}. Note, however, that τ_{lung} and G_{lung} will vary, depending on the steady-state operating levels of $\dot{V}_E$ and P_{aCO_2}. This reflects the

fundamentally *nonlinear* nature of the gas exchange process. Another important detail is that the negative value for $H_{lung}(s)$ in Equation (6.44) merely implies that the negative feedback in this closed-loop system is embedded in the CO_2 exchange process (i.e., when ventilation increases, P_{aCO_2} decreases). G_{lung} will always be positive since P_{aCO_2} must be greater than P_{ICO_2} (for positive metabolic CO_2 production rates).

6.7.2 Transport Delays

We assume that pulmonary end-capillary blood returning to the heart will take some time (T_p) to arrive at the peripheral chemoreceptors (carotid bodies) and a slightly longer time ($T_c > T_p$) to first appear at the site of the central (medullary) chemoreceptors. Thus,

$$\Delta P_{pCO_2}(t) = \Delta P_{aCO_2}(t - T_p) \tag{6.47a}$$

$$\Delta P_{cCO_2}(t) = \Delta P_{aCO_2}(t - T_c) \tag{6.47b}$$

All mixing effects in the vasculature during the convective process are ignored. The Laplace transforms corresponding to Equations (6.47a) and (6.47b) are

$$\Delta P_{pCO_2}(s) = e^{-sT_p}\Delta P_{aCO_2}(s) \tag{6.48a}$$

$$\Delta P_{cCO_2}(s) = e^{-sT_c}\Delta P_{aCO_2}(s) \tag{6.48b}$$

6.7.3 Controller Responses

Following Bellville et al. (1979), we assume the following dynamic relations for the peripheral and central chemoreflex responses:

$$\tau_p \frac{d\dot{V}_p}{dt} + \dot{V}_p = G_p[P_{pCO_2} - I_p] \tag{6.49a}$$

$$\tau_c \frac{d\dot{V}_c}{dt} + \dot{V}_c = G_c[P_{cCO_2} - I_c] \tag{6.49b}$$

and

$$\dot{V}_c + \dot{V}_p = \dot{V}_E \tag{6.49c}$$

In the above controller equations, τ_p and τ_c represent the characteristic response times of the peripheral and central chemoreflexes, respectively; it is assumed that $\tau_c \gg \tau_p$. G_p and G_c represent the steady-state gains for the peripheral and central controllers, respectively. The square brackets on the right-hand side of Equations (6.49a) and (6.49b) are used to imply a thresholding operation: i.e., these terms will be set equal to zero if the quantities within the brackets become negative. Thus, I_p and I_c represent the corresponding apneic thresholds for the peripheral and central chemoreceptors, respectively.

Assuming that the "set-point" of operation is nowhere in the vicinity of the apneic thresholds, Equations (6.49a) and (6.49b) can be linearized using small-signal analysis. The result of this analysis following Laplace transformation yields:

$$\Delta \dot{V}_p(s) = \frac{G_p}{\tau_p s + 1} \Delta P_{pCO_2}(s) \tag{6.50a}$$

$$\Delta \dot{V}_c(s) = \frac{G_c}{\tau_c s + 1} \Delta P_{cCO_2}(s) \tag{6.50b}$$

6.7.4 Loop Transfer Functions

Corresponding to the two feedback loops in this model are two loop transfer functions: one for the peripheral chemoreflex loop ($H_{Lp}(s)$) and the other for the central chemoreflex loop ($H_{Lc}(s)$). These are derived by combining Equations (6.44), (6.48a), and (6.50a):

$$H_{Lp}(s) \equiv \frac{\Delta \dot{V}_p(s)}{\Delta \dot{V}_E(s)} = \frac{G_{lung} G_p e^{-sT_p}}{(\tau_{lung} s + 1)(\tau_p s + 1)} \tag{6.51a}$$

$$H_{Lc}(s) \equiv \frac{\Delta \dot{V}_c(s)}{\Delta \dot{V}_E(s)} = \frac{G_{lung} G_c e^{-sT_c}}{(\tau_{lung} s + 1)(\tau_c s + 1)} \tag{6.51b}$$

Since the overall frequency response of the loop transfer function is defined as

$$H_L(\omega) \equiv \frac{\Delta \dot{V}_p(\omega) + \Delta \dot{V}_c(\omega)}{\Delta \dot{V}_E(\omega)} \tag{6.52}$$

if we combine Equations (6.51a) and (6.51b) and introduce the substitution $s = j\omega$, we obtain the following expression for the overall frequency response of the two loops:

$$H_L(\omega) = \frac{G_{lung}}{(1 + j\omega\tau_{lung})} \left(\frac{G_p e^{-j\omega T_p}}{(1 + j\omega\tau_p)} + \frac{G_c e^{-j\omega T_c}}{(1 + j\omega\tau_c)} \right) \tag{6.53}$$

Thus, the stability of the respiratory control model for a given set of parameters (V_{lung}, Q, K_{CO_2}, G_p, τ_p, G_c, τ_c) and conditions ($\dot{V}_E$, P_{aCO_2}, P_{ICO_2}) can be tested by applying the Nyquist criterion to Equation (6.53).

6.7.5 Nyquist Stability Analysis Using MATLAB

The generation of the Nyquist diagram from Equation (6.53) can be carried out relatively easily using MATLAB. The following shows sample lines of MATLAB code that can be used for this purpose.

```
>>% Construct loop transfer functions
>> num1 = [Glung*Gp]; den1 = [taulung*taup  (taulung + taup)  1];
>> Hs1 = tf(num1, den1);
>> num2 = [Glung*Gc]; den2 = [(taulung*tauc)  taulung +tauc)  1;
>> Hs2 = tf(num2, den2);

>>% Compute Nyquist results, excluding effect of pure delays
>> [R1, I1] = nyquist(Hs1, w); R1 = squeeze(R1); I1 = squeeze(I1);
>> [R2,I2] = nyquist(Hs2, w);R2 = squeeze(R2); I2 = squeeze(I2);

>>% Add delay to results
>> R1del = real((R1 + j*I1).*exp(-j*w*Tp));
>>I1del = imag((R1 + j*I1).*exp(-j*w*Tp));
>> R2del = real((R2 + j*I2).*exp(-j*w*Tc));
>> I2del = imag((R2 + j*I2).*exp(-j*w*Tc));
>> Rdel = R1del + R2del;
>> Idel = I1del + I2del;

>>% Plot Nyquist diagram of overall frequency response
>> axis square; plot(Rdel,Idel); grid;
```

Figure 6.16 shows Nyquist plots representing the overall frequency responses in the case of the typical normal subject (N) and the patient with congestive heart failure (C). We have assumed the following parameter values to represent *both* types of subjects: $V_{lung} = 2.5\,\text{L}$, $K_{CO_2} = 0.0065\,\text{mm Hg}^{-1}$, $G_p = 0.02\,\text{L s}^{-1}\,\text{mm Hg}^{-1}$, $G_c = 0.04\,\text{L s}^{-1}$

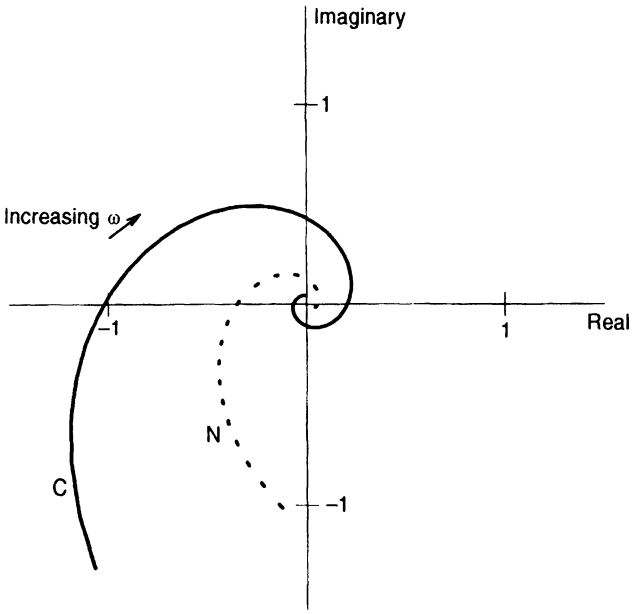

Figure 6.16 Nyquist plots representing the frequency responses of the linearized ventilatory control model in the normal subject (N, dotted curve) and patient with congestive heart failure (C, continuous curve). Frequencies represented in plots range from 0.01 to 0.1 Hz.

mm Hg^{-1}, $\tau_p = 20\,\text{s}$, $\tau_c = 120\,\text{s}$, $\dot{V}_E = 0.12\,\text{L s}^{-1}$, $\dot{V}_D = 0.03\,\text{L s}^{-1}$, $P_{ICO_2} = 0$, and $P_{aCO_2} = P_{ACO_2} = 40\,\text{mm Hg}$. In the normal subject, the following circulatory parameter values were assigned: $T_p = 6.1\,\text{s}$, $T_c = 7.1\,\text{s}$, and $Q = 0.1\,\text{L s}^{-1}$. In the patient with congestive heart failure, we assumed a halving of cardiac output and a doubling of the circulatory delays: $Q = 0.05\,\text{L s}^{-1}$, $T_p = 12.2\,\text{s}$, and $T_c = 14.2\,\text{s}$. The MATLAB script file ("`nyq_resp.m`") used to generate the Nyquist plots shown is included with the set of MATLAB/SIMULINK files that accompany this book.

The Nyquist plots in Figure 6.16 represent a bandwidth of frequencies that range from 0.01 to 0.1 Hz. These correspond to interbreath periodicities of cycle durations 10 to 100 s. In the normal subject (N), the Nyquist plot shows a stable system with a critical loop gain (i.e., at $-180°$) of 0.34. This critical point occurs at $f = 0.0295\,\text{Hz}$ or the equivalent of a periodicity of 34 s. Thus, when transient oscillations in ventilation appear in the normal subject, we would expect these oscillations to have a cycle duration of 34 s. On the other hand, in the subject with congestive heart failure, the halving of Q and doubling of circulatory delays lead to a rotation and stretching of the Nyquist locus. Since the locus encircles the $(-1 + j0)$ point, we can conclude that under the assigned conditions, this system is unstable. The loop gain at $-180°$ is now 1.02, with the critical frequency occurring at $f = 0.0165\,\text{Hz}$, which is equivalent to a periodicity of approximately 61 s. These cycle durations are consistent with the oscillation periods that have been observed in normals and heart failure subjects who exhibit Cheyne–Stokes respiration. For more complicated models and analyses, the reader is referred to journal reports such as those published by Khoo et al. (1982), Carley and Shannon (1988), and Nugent and Findley (1987).

BIBLIOGRAPHY

Bellville, J.W., B.J. Whipp, R.D. Kaufman, G.D. Swanson, K.A. Aqleh, and D.M. Wiberg. Central and peripheral chemoreflex loop gain in normal and carotid body-resected subjects. *J. Appl. Physiol.* **46**: 843–853, 1979.

Carley, D.W., and D.C. Shannon. A minimal mathematical model of human periodic breathing. *J. Appl. Physiol.* **65**: 1400–1409, 1988.

Clynes, M. Computer dynamic analysis of the pupil light reflex. *Proc. 3d Int. Conf. Med. Electron.* International Federation of Medical Electronics and Biomedical Engineering, and Institute of Electrical Engineers (London), 1960, pp. 356–358.

Dorf, R.C., and R.H. Bishop. *Modern Control Systems*, 7th ed. Addison-Wesley, Reading, MA, 1995.

Khoo, M.C.K., R.E. Kronauer, K.P. Strohl, and A.S. Slutsky. Factors inducing periodic breathing in humans: a general model. *J. Appl. Physiol.* **53**: 644–659, 1982.

Llaurado, J.G., and H.H. Sun. Modified methods for studying stability in biological feedback control systems with transportation delays. *Med. Electron. Biol. Eng.* **2**: 179–184, 1964.

Nugent, S.T., and J.P. Finley. Periodic breathing in infants: a model study. *IEEE Trans. Biomed. Eng.* **34**: 482–485, 1987.

Stark, L. Stability, oscillations, and noise in the human pupil servomechanism. *Proc. I.R.E.* **47**: 1925–1939, 1959.

PROBLEMS

P6.1. Figure P6.1 shows a simple negative feedback control system with a variable gain, K, in the feedback element. Determine the smallest value of K that would render this closed-loop system unstable, using (a) the Routh–Hurwitz test and (b) the Nyquist stability criterion.

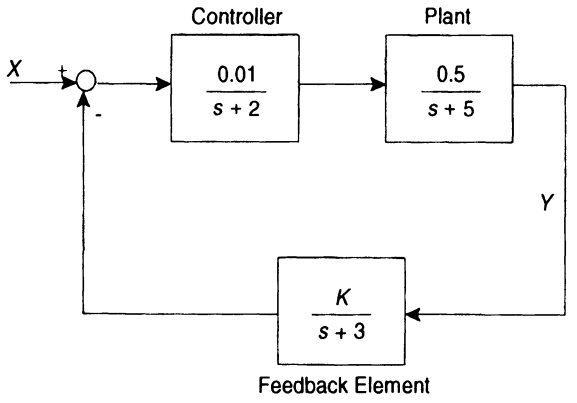

Figure P6.1 Simple control system with variable feedback gain.

P6.2. Consider the simple model of eye-movement control shown schematically in Figure P4.1. Assume that $G/J = 14\,400\,\text{rad}^2\,\text{s}^{-2}$, $B/J = 24\,\text{rad}\,\text{s}^{-1}$.
(a) If $k_v = 0.01$, deduce the gain and phase margins of this closed-loop system.
(b) Using the Routh–Hurwitz and Nyquist stability tests, determine the value of k_v at which you might expect the model to exhibit self-sustained oscillations in θ.

P6.3. In the model of ventilatory control with feedback from the intrapulmonary CO_2 receptors shown in Figure P4.3, determine how rate sensitivity is expected to affect relative stability. Compute the gain and phase margins of this system, and display the corresponding Bode diagrams, when the rate sensitivity factor, α, assumes the following values: (a) $\alpha = 0$; (b) $\alpha = \frac{1}{2}$; and (c) $\alpha = 2$.

P6.4. In the analysis of the pupillary light reflex model discussed in Section 6.6, the transfer function representing the pure delay, D, was approximated as a power series in the Laplace variable s. Repeat the Routh–Hurwitz and Nyquist stability analyses, assuming a first-order Padé approximation to the delay, i.e., assume that

$$e^{-sD} = \frac{1 - \frac{Ds}{2}}{1 + \frac{Ds}{2}}$$

In each case, find the value of the steady-state loop gain, K, that would lead to the production of self-sustained oscillations in pupil diameter.

P6.5. Consider the neuromuscular reflex model of Figure 4.11. Develop a MATLAB program that would enable you to assess the relative stability of this model as the feedback gain, β, is changed. Assume the following values for the rest of the model parameters: $J = 0.1\,\text{kg}\,\text{m}^2$, $k = 50\,\text{N}\,\text{m}$, $B = 2\,\text{N}\,\text{m}\,\text{s}$, $\tau = 1/300\,\text{s}$, $T_d = 0.02\,\text{s}$, and $\eta = 5$. Determine whether your prediction of the critical value of β for instability to occur is compatible with simulation results using the SIMULINK program "`nmreflex.mdl`."

P6.6. It is known that hyperoxia, induced by breathing a gas mixture with high O_2 content, can substantially attenuate the CO_2 sensitivity of the peripheral chemoreceptors. As a first approximation, we can assume that this sets the parameter G_p in the chemoreflex model of Section 6.7 equal to zero. This effectively reduces the model to only one feedback loop—that involving the central chemoreflex. Employing Routh–Hurwitz and Nyquist stability analyses, show that administration of inhaled O_2 would eliminate Cheyne–Stokes breathing in the patient with congestive heart failure. Use the parameter values given in Section 6.7.5.

P6.7. Develop a SIMULINK representation of the chemoreflex model described in Section 6.7, using the parameter values pertinent to the normal subject. Investigate the stability of the SIMULINK model by introducing impulsive perturbations into the closed-loop system.

Determine how changes in the following model parameters may promote or inhibit the occurrence of periodic breathing: (a) V_{lung}, (b) P_{ICO_2}, (c) G_c, and (d) G_p. Verify your conclusions using the Nyquist analysis technique illustrated in Section 6.7.